Conserved Properties of Genetic Architecture of Renal and Fat Transcriptomes in Rat Models of Insulin Resistance

Georg W Otto[1]*, Pamela J. Kaisaki[2]*, Francois Brial[3], Aurélie Le Lay[3], Jean-Baptiste Cazier[4], Richard Mott[5], Dominique Gauguier[2,3,6]

[1] Genetics and Genomic Medicine, University College London Institute of Child Health, 30 Guilford Street, London WC1N 1EH, United Kingdom

[2] The Wellcome Trust Centre for Human Genetics, University of Oxford, Roosevelt Drive, Headington, Oxford OX3 7BN, United Kingdom

[3] University Paris Descartes, INSERM UMR 1124, 45 rue des Saint-Pères, 75006 Paris, France

[4] Centre for Computational Biology, Medical School, University of Birmingham, Birmingham, United Kingdom

[5] University College London Genetics Institute, Gower Street, London WC1E 6BT, United Kingdom

[6] McGill University and Genome Quebec Innovation Centre, 740 Doctor Penfield Avenue, Montreal, QC, H3A 0G1, Canada

* Equivalent contribution

Correspondence should be addressed to D.G. (Tel: +33 14427156, Fax: +33 14427162, e-mail: dominique.gauguier@inserm.fr).

Key Words: eQTL, Goto-Kakizaki Rat, Diabetes Mellitus, Genetic Crosses, Insulin Resistance, Quantitative Trait Locus, SHR, Single Nucleotide Polymorphism, Spontaneously Hypertensive rat, Systems Genetics, Transcriptome.

Summary statement

Kidney and fat expression QTL mapping in rat models of spontaneously-occurring insulin resistance associated with either diabetes or hypertension reveals conserved gene expression regulation suggesting shared etiology of disease phenotypes.

Abstract

To define renal molecular mechanisms that are affected by permanent hyperglycemia and may promote phenotypes relevant to diabetes nephropathy, we carried out linkage analysis of genome-wide gene transcription in kidney of F2 offspring from the Goto-Kakizaki (GK) rat model of type 2 diabetes and normoglycemic Brown Norway (BN) rats. We mapped 2526 statistically significant expression quantitative trait loci (eQTLs) in the cross. Over 40% of eQTLs mapped in the close vicinity of the linked transcripts, underlying possible cis-regulatory mechanisms of gene expression. We identified eQTL hotspots on chromosomes 5 and 9 regulating the expression of 80-165 genes, sex or cross direction effects, and enriched metabolic and immunological processes by segregating GK alleles. Comparative analysis with adipose tissue eQTLs in the same cross showed that 496 eQTLs, as well as top enriched biological pathways, are conserved in the two tissues. Extensive similarities in eQTLs mapped in the GK and in the spontaneously hypertensive rat (SHR) suggest a common etiology of disease phenotypes common to the two strains, including insulin resistance which is a prominent pathophysiological feature in both GK and SHR. Our data shed light on shared and tissue specific molecular mechanisms that may underlie etiological aspects of insulin resistance in the contexts of spontaneously occurring hyperglycemia and hypertension.

Introduction

Transcriptome-based molecular phenotyping provides detailed information on the expression of individual genes and biological pathways. Variation in transcript abundance can be mapped to the genome at expression quantitative trait loci (eQTL). The genetic control of gene transcription in mammals has been reported in various organs from preclinical models of human chronic diseases using experimental crosses (Davis et al., 2012; Kaisaki et al., 2016; van Nas et al., 2010), recombinant congenic strains (Hubner et al., 2005; Petretto et al., 2006), congenic strains (Dumas et al., 2016; Kaisaki et al., 2016) recombinant congenic strains (Lee et al., 2006) and mice of the collaborative cross (Aylor et al., 2011). eQTL mapping in humans has progressed from whole blood and cell systems (Dixon et al., 2007; Fairfax et al., 2012; Grundberg et al., 2012) to multiple post-mortem organs in control individuals (Battle et al., 2017), which were used to identify genes and biological pathways causing chronic diseases through computational integration with genome wide association study (GWAS) data (Gamazon et al., 2018).

However, this strategy does not account for expected organ-specific variation in gene expression in disease conditions, which require access to biopsies from the affected tissues that are often impossible to collect in large groups of phenotypically homogeneous patients and healthy controls. In addition, the genetic basis of several diseases remains poorly characterised through GWAS. Diabetes nephropathy is a typical example of a complex genetic disease condition where causative genes have not been robustly mapped in humans through GWAS (Ahlqvist et al., 2015) and where the identification of contributing molecular mechanisms is therefore essential. These limitations underline the importance of preclinical models of human chronic diseases to accurately define tissue specific genetic control of gene transcription in standardised experimental conditions.

The Goto-Kakizaki (GK) rat is a model of type 2 diabetes mellitus, which spontaneously exhibits biochemical and histological evidence of nephropathy (Janssen et al., 2004). It was produced over many generations of breeding outbred Wistar rats using glucose intolerance as the sole criterion for selecting breeders (Goto et al., 1976) in order to progressively enrich the genome of offspring in naturally occurring polymorphisms contributing to impaired glucose homeostasis, whilst integrating alleles promoting increased susceptibility, as well as possibly resistance, to diabetes endophenotypes and associated complications (Bihoreau et al., 2017). We and others have derived intercrosses between GK and normoglycemic Brown Norway (BN) rats to comprehensively map genes responsible for the control of glucose tolerance, insulin secretion and adiposity (Gauguier et al., 1996), islet morphology (Finlay et al., 2010), lipid metabolism (Argoud et al., 2006), proteinuria (Nobrega et al., 2009), plasma metabolomic variables (Dumas et al., 2007) and adipose tissue gene transcription (Kaisaki et al., 2016).

Here, we characterised the genetic architecture of renal gene expression in chronic diabetes through the mapping of kidney eQTL in a GKxBN F2 cross. We identified similarities in the genetic architecture of gene transcription regulation in kidney and adipose tissue and conserved eQTL genes in the GK and spontaneously hypertensive rat (SHR), suggesting common molecular mechanisms and shared genetic etiology of pathophysiological phenotypes. These data provide detailed information of genomic regulation in the diabetic kidney which can point to individual genes and biological pathways involved in the etiopathogenesis of human diabetic nephropathy and insulin resistance.

Methods

Animals

The GKxBN F2 cross (n=123) previously derived to map QTLs for pathophysiological phenotypes (Gauguier et al., 1996), metabolomic variables (Dumas et al., 2007) and adipose tissue eQTLs (Kaisaki et al., 2016) was used for kidney eQTL mapping. The cohort consisted of 60 males and 63 females generated from two reciprocal crosses of 55 F2 rats originating from a GK female and 68 F2 rats originating from a BN female (Figure 1). At six months, animals were fasted overnight and killed by terminal anaesthesia. The right kidney was isolated, snap frozen in liquid nitrogen and stored at -80C until RNA preparation.

RNA preparation

Total RNA was prepared from 100mg of frozen kidney using the RNeasy® 96 Universal Tissue kit (Qiagen, Crawley, UK) as previously described (Kaisaki et al., 2016). Frozen tissue samples were homogenised in QIAzol Lysis Reagent using Qiagen's Tissue Lyser. Total RNA was purified and eluted in 90µl of RNase-free water. RNA concentrations were determined using a NanoDrop spectrophotometer and RNA integrity was assessed using an Agilent 2100 Bioanalyser (Agilent Technologies, Waldbronn, Germany).

Illumina Bead Array hybridisation, scanning and data processing

Kidney gene transcription profiling was performed as previously described (Kaisaki et al., 2016) using Sentrix®BeadChipRatRef-12v1 Whole-Genome Gene Expression Arrays (Illumina Inc., San Diego, CA), which contain 22,523 oligonucleotide probes (replicated on average 30 times) allowing quantification of transcript levels for 21,910 genes. Double-stranded cDNA and purified biotin-labelled cRNA were synthesised from 300ng high quality total RNA using the Illumina®TotalPrep RNA amplification kit (Ambion Inc., Austin, TX). cRNA concentrations were determined using a NanoDrop spectrophotometer and cRNA quality and integrity were assessed on an Agilent 2100 Bioanalyser (Agilent Technologies,

Waldbronn, Germany). 750ng of each biotinylated cRNA was used for hybridisation onto the arrays. BeadChip arrays were scanned on the Illumia® Bead Array Reader (Illumina Inc., San Diego, CA) and data were analysed using the Illumina® Bead Studio Application software before undergoing comprehensive statistical analysis. Quality control parameters were: $0 \leq$ G sat ≤ 1; Green 95 Percentile (GP95) for consistency between arrays (around 2000); GP5 background level in range of low 100 or below. Prior to array analysis, data from 757 Illumina oligonucleotides, which carry DNA variants between GK and BN (Kaisaki et al., 2016) were removed. We also withdrew probes that detected only background signal (ie. Illumina detection score <0.5 in >50% of samples). Microarray data processing was carried out using normexp background correction and quantile normalization (Shi et al., 2010).

Microarray experiments were compliant with MIAME (Minimum Information About a Microarray Experiment) and both protocol details and raw data have been deposited in ArrayExpress (http://www.ebi.ac.uk/arrayexpress/) under the accession number E-MTAB-969.

Genetic mapping of expression QTLs in the F2 (GKxBN) cross

eQTL analysis was performed using the R-qtl software package (Broman et al., 2003) as previously described (Kaisaki et al., 2016) based on genetic maps constructed in the cross (Wilder et al., 2004). The Haley-Knott regression method was used for genome scans (Haley and Knott, 1992). We used sex and cross direction as additive covariates in our models to account for effects of sex and lineage on gene expression (Solberg et al., 2004). Permutation tests (n=1,000) were carried out to determine genome wide significance threshold for each transcript. QTLs with a genome-scan adjusted p-value <0.05 were considered as significant.

Regression model with sex and cross direction as additive covariants was as in (Kaisaki et al., 2016). To detect sex x genotype interactions, QTL mapping analyses were also carried out using regression models containing sex as interactive covariates.

$$(H_i) \quad y_i = \mu + \beta_c c_i + \beta_s s_i + \beta_g g_i + \gamma s_i g_i + \varepsilon_i$$

With $\beta_c c_i$ denoting the effect of the cross, $\beta_s s_i$ denoting the effect of sex, $\beta_g g_i$ denoting the effect of the genotype and $\gamma s_i g_i$ denoting the interaction of sex x genotype. To obtain evidence for interactions between QTLs and sex, *Hi* was compared to the additive model *Ha*. This results in LOD_f:

$$LOD_f = LOD_i - LOD_a$$

To detect cross x genotype interactions (cross direction effects, CDE), we included cross direction as an interaction term.

Pathway analyses

Pathway analyses of transcriptome data were performed as previously described (Kaisaki et al., 2016) to determine functional categories enriched in the eQTL-controlled genes in the F2 cross. A hypergeometric test was used on gene ontology terms and KEGG pathways associated with gene sets against the background of genes with detectable expression (Falcon and Gentleman, 2007).

Results

Genetic mapping of genome-wide gene transcription control in the diabetic kidney in (GKxBN) F2 rats

We have previously shown that adult rats (7 month-old) of our GK colony exhibit varying degrees of thickening of the glomerular basement membrane and mild mesangial extracellular matrix expansion when compared to normoglycemic BN controls (Wallis et al., 2008). To characterise the architecture of renal gene transcription that may account for these renal structural changes and for proteinuria that segregates in a GKxBN F2 cross (Nobrega et al., 2009), we applied an eQTL strategy to map genetic loci linked to quantitative variations in the abundance of renal transcripts in the GKxBN F2 offspring previously used for diabetes

QTL analysis (Gauguier et al., 1996). Genotypes at over 255 framework markers typed in the cross were used to impute allele probabilities and construct a map of 898 marker positions (2.5 cM spacing between markers). These were used to test for linkage to detectable Illumina array signals in each of the 123 F2 rats as previously described (Kaisaki et al., 2016). Genome sequencing of the GK/Ox strain (Atanur et al., 2013) allowed us to exclude data from Illumina oligonucleotides for 757 genes containing genetic polymorphisms between GK and BN (Kaisaki et al., 2016), which may alter binding between probes and the oligonucleotides (Alberts et al., 2007), resulting in spurious eQTLs or questionable lack of genetic linkage to the corresponding transcripts. As previously observed in adipose tissue eQTLs mapped in the same cross (Kaisaki et al., 2016), over 40% of probes with DNA polymorphisms gave significant eQTL signals (LOD>10), which deviated from the distribution eQTL significance when all oligonucleotides were considered (Figure 2). After filtering out probes with low intensity signal a total of 15759 transcripts were considered for linkage analyses.

We identified a total of 2526 eQTLs at FDR<0.05 (Table 1), including 2252 (89%) linked to transcripts localised to a single genomic position in the rat genome assembly (RGSC3.4, Ensembl release 69) (Table S1). Analysis of eQTL statistical significance showed that 509 eQTLs (20.1%) can be detected with high confidence (LOD>10) (Figure 3A, Table S1). Chromosome distribution of eQTLs showed that 11% of genes on average on each chromosome were regulated by eQTLs in the cross (Table 1). An excess of eQTLs was detected on chromosomes 5 (27% of genes were associated with an eQTL) and 9 (23% of genes were associated with an eQTL) (Table 1).

Genetic mapping of local and distant renal gene transcription regulation in (GKxBN) F2 rats

To assess gene transcription regulation through cis- and trans-mediated genetic effects, we compared the genomic positions of transcripts and linked marker loci showing the strongest evidence of significant linkage (Figure 3B). A total of 1141 eQTLs (46%) accounted for linkage between markers and transcripts mapped to different chromosomes, which unambiguously underlie trans-mediated mechanisms of gene transcription regulation (Table 1; Table S1). The remaining 1356 eQTLs mapped to chromosomes where the linked transcripts were encoded, including 1283 eQTLs linked to genes assigned to a unique position in the rat genome assembly. A high proportion of these eQTLs were within 10Mb (n=1029, 80.3%) or 5Mb (n=788, 61.4%) of the linked transcripts, which could underlie *cis*-regulatory mechanisms of gene transcription (Figure 3B, Table S1). The mean LOD score for statistically significant eQTLs was 8.32±8.65 (SD) and there was an inverse relationship between eQTL significance and frequency (Figure 3C). eQTLs localised in the close vicinity to the linked transcripts, which are most likely regulated in *cis*, showed the highest proportion of statistically significant linkage (Figure 3D). Polygenic control of the expression of 133 genes was suggested when two or more eQTLs were linked to the same gene (Table S1).

Kidney eQTLs were generally evenly distributed across the genome (Figure 3E). However, we noted an excess of *trans*-mediated eQTLs on chromosomes 5 (n=252) and 9 (n=111), which accounts for the above mentioned high number of eQTLs on chromosomes 5 (n=379) and 9 (n=175) (Table 1). This can be explained by eQTL clustering in regions of chromosomes 5 (50-55cM; 120.3-132.3Mb) and 9 (79.5-84.5cM; 99.2-104.4Mb), which control the expression of 165 genes (chromosome 5 eQTLs) and 80 genes (chromosome 9 e QTLs) generally regulated in *trans* (Figure 3E; Table S1). GK genotypes at the eQTL hotspot

on chromosome 5 were predominantly associated with downregulated expression of an important proportion of eQTL genes (129/165; 78%), suggesting that this phenomenon may have genuine biological relevance and reflect the existence of a master regulator of gene transcription at this locus.

Genetic analysis of the renal gene transcriptome identifies sex and cross direction effects

The design of the experimental cross combining male and female F2 hybrids originating from GK females or GK males (Figure 1) allowed us to detect sex and cross direction specific patterns of gene expression for 516 and 209 kidney eQTLs, respectively (Table 1; Table S2). eQTLs showing cross direction effects (CDE) were evenly distributed across the genome (Figure 3F,G) with an average frequency of 0.9% of genes impacted by CDE, and few were highly significant (maximum interactive LOD = 20.4) (Table 1; Table S2). Even though parent-of-origin effects, which may account for parental imprinting, cannot be assessed in our experimental setting of an F2 cross, several eQTLs showing evidence of CDE in the GKxBN F2 cross were linked to imprinted genes, including *Igf2* (LOD = 4.58, P=0.001), *Ndn* (LOD = 4.81, P<0.001), *Zfat* (LOD = 5.52, P<0.001), *Tp53* (LOD = 4.85, P<0.001) and *Cdk4* (LOD = 2.93, P=0.049). Interestingly, expression of *Igf2*, *Ndn* and *Tp53* was regulated by CDE eQTLs in the same region of chromosome 2 (98.9-103.9cM), suggesting the existence of a regulator of gene imprinting in this region.

In contrast to CDE eQTLs, instances of strongly significant linkages were found for sex-specific eQTL effects (maximum interactive LOD = 104.7) (Table S2). Sex-specific and CDE eQTLs were mutually exclusive. Only one locus on chromosome 4 exhibited both sex-specific effects (LOD = 3.04) and CDE (LOD = 2.92) *trans*-mediated linkage with the gene *Trak2*. Few eQTLs detected in the full F2 population combining both males and females showed evidence of significant CDE (*Akr1c2*, *Dbndd1*, *F2*, *Ptpro*). In contrast, a relatively large number of sex-specific eQTLs, generally regulated in *cis* were also significant in the

full F2 population (*Akr1b7*, *Ank2*, *Armc3*, *Ifitm6*, *LOC494499*, *LOC500300*, *LOC684289*, *Neurl2*, *Nfkbia*, *Pou4f1*, *RGD1309350*, *RGD1559948*, *RGD1562107*, *RGD1563820*, *RGD1564419*, *RGD1564696*, *RGD1565387*, *RGD1566401*, *Scgb1c1*, *Slc22a13*, *Sparcl1*, *Spink8*, *Tgfb2*).

The vast majority of eQTLs showing CDE were unambiguously mediated in *trans* (Figure 3G), whereas the most significant sex-specific eQTLs (LOD>10) were predominantly linked to genes mapped to the same chromosome (25/30; 83%) and often localised in the close vicinity (<10Mb) of linked transcripts (19/30; 63%), suggesting *cis*-mediated gene expression regulation (Table S2). Sex-specific eQTLs were found on all rat chromosomes (Figure 3H) with an average of 2.2% showing such effect across the genome (Table 1). However, when gene density of individual chromosome was considered, we noted a much stronger proportion of genes showing a sex-specific eQTL pattern on chromosomes 5 (n=116; 8.3%), 9 (n=90; 11.8%) and 17 (n=65; 9.3%) (Table 1; Table S2). Overall, 52.6% of sex-specific eQTLs were localised on chromosomes 5 (22.5%), 9 (17.5%) and 17 (12.6%) (Table 1; Table S2; Figure 3H) and were organised in clusters in the centromeric and interstitial regions of chromosome 5 (0-2.5cM, 0-5.8Mb, n=27 and 25-32.5cM, 53.1-68.2Mb, n=53), at the telomeric end of chromosome 9 (69.9-84.5cM, 90.5-104.4Mb, n=71) and in the interstitial regions of chromosome 17 (36.1-48.6cM, 53.0-80.2Mb, n=45) (Figure 3I; Table S2). GK alleles at the sex-specific eQTLs in the centromeric region of chromosome 5 (0-2.5cM) were predominantly associated with upregulated gene expression (21/27), whereas they were associated with downregulated gene expression on chromosome 9 (47/71).

eQTL-based pathway analysis underscores the involvement of immunological processes and drug metabolism in the diabetic kidney

To identify biological consequences of diabetes and segregating GK/BN polymorphisms across the rat genome on renal transcriptional changes, we carried out pathway enrichment

analysis of genes under eQTL control in F2 hybrids. A total of 40 biological pathways were significantly altered, including primarily mechanisms related to drug and xenobiotic metabolism by cytochrome P450 and also various immunological functions covering autoimmune diseases (thyroid and graft versus host diseases, type 1 diabetes, rheumatoid arthritis) and cellular immune and inflammatory processes (e.g. antigen processing and presentation, phagosome) (Table 2). Metabolic pathways were also significantly affected, including bile acids, pentose and glucuronate, amino acids (alanine, aspartate, glutamate, valine, leucine, isoleucine, selenocompounds), arachidonic acid, butanoate, ketone bodies and vitamins (ascorbate, vitamin B6, retinol, folate). Altered processes related to cell adhesion, O-glycan biosynthesis and nitrogen metabolism may contribute to impaired renal structural and functional regulation.

eQTL genes contributing to the top ranking pathway (drug metabolism, KEGG 982) included aldehyde oxidases (*Aox1*, *Aox3l1*), cytochromes P450 (*Cyp2c11*, *Cyp2d1*, *Cyp2d4*, *Cyp2d5*, *Cyp2e1*), flavin containing monooxygenases (*Fmo1*, *Fmo2*, *Fmo4*, *Fmo5*), glutathione S-transferases (*Gsta4*, *Gsta5*, *Gstm2*, *Gstm4*, *Gstp1*, *Gstt1*, *Gstt2*) and UDP glucuronosyltransferases (*Ugt1a1*, *Ugt1a7c*, *Ugt2b10*, *Ugt2b15*, *Ugt2b17*, *Ugt2b37*) (Table S1). The eQTL genes for these glutathione S-transferases and several UDP glucuronosyltransferases also accounted for the enrichment of the metabolism of xenobiotics by cytochrome P450 pathway (KEGG 980), and eQTL genes for these cytochromes P450 and these UDP glucuronosyltransferases contributed to the retinol metabolism pathway (KEGG 830).

eQTLs linked to RT1 class I and II genes (*RT1-A2*, *RT1-CE5*, *RT1-CE10*, *RT1-CE15*, *RT1-CE16*, *RT1-Da*, *RT1-DMa*, *RT1-DMb*, *RT1-Ha*, *RT1-M3-1*, *RT1-M10-1*, *RT1-N2*, *RT1-N3*, *RT1-CE5*) dominated the enrichment of the antigen processing and presentation pathway (KEGG 4612). eQTLs for all these RT1 genes, along with *RT1-T24-4*, lysosomal H^+

transporting ATPases (*Atp6ap1*, *Atp6v0a4*, *Atp6v0e1*, *Atp6v1d*, *Atp6v1g3*) and tubulins (*Tuba4a*, *Tubb2b*, *Tubb3*, *Tubb5*) accounted for the enrichment of the phagosome pathway (KEGG 4145).

Results from our genome-wide functional analysis of the genetic control of renal gene transcription provide a comprehensive landscape of altered biological functions in the diabetic kidney and underline the high level of complexity of coordinated regulations of molecular processes contributing to renal pathological mechanisms in diabetes in the GK rat.

Kidney and adipose tissue transcriptomes exhibit tissue specific eQTL features

To investigate biological functions consistently affected in different tissues in diabetes in the GK rat, we compared architectural and functional features of kidney eQTLs to previously reported adipose tissue eQTLs mapped in animals of the same GKxBN F2 cross using strictly identical experimental and analytical procedures (Kaisaki et al., 2016). We identified approximately the same number of eQTLs in kidney (2526) and adipose tissue (2735) in the cross (Table S3). Hotspots of eQTLs mostly mediated in *trans* were identified in both tissues, but they were detected on different chromosomes in adipose tissue (chromosomes 1, 7 and 17) and kidney (chromosome 9), and in different regions of chromosome 5 in adipose tissue (57.5–62.5cM) and kidney (0-2.5cM and 25-32.5cM). At the gene level, nearly 20% (496/2526, $p = 6 \times 10^{-4}$, one-sided Fisher's Exact Test) of predominantly locally regulated (n=414) kidney eQTLs, were also significant in adipose tissue in the cross (ie. eQTL mapped within 15cM in the two tissues and consistent allelic effect on gene expression changes), which reveal conserved molecular mechanisms in the two tissues. There were good correlations between kidney and adipose tissue for both the magnitude of the allelic effects (Figure 4A) and LOD scores (Figure 4B) at the common eQTLs. In contrast, only few genuine *trans*-mediated eQTLs were conserved in the two tissues (Table S4).

Sex-effects and CDE were also observed in adipose tissue eQTLs (Table S3). However, we did not identify strong excess of sex-specific adipose tissue eQTLs on any chromosome in contrast to our observation on chromosomes 5 and 9 in kidney. In the vast majority of cases sex-specific and CDE eQTLs identified in the adipose tissue trancriptome were mutually exclusive (Table S5). Only 10 genes showed both sex-effects and CDE (*Gper*, *Olr241*, *LOC501102*, *LOC501113*, *Ppic*, *Ppp4c*, *RGD1564266*, *Rtp3*, *Setdb2*, *Wdr24*), but only two (*Gper*, *LOC501113*) were controlled by the same locus. Conserved sex- and cross direction-specific genetic effects in fat and kidney was observed for only 11 and 10 genes, respectively, but the location of the eQTLs was consistent for only two genes (*Nfkbia*, *Rai14*) for sex effect and one gene (*Tarsl2*) for cross direction effects (Tables S2 and S5).

eQTLs drive tissue-specific functional enrichment in kidney and adipose tissue

To identify organ-specific and shared genetic regulation of biological pathways in diabetes transcriptomes, we compared results from GSEA of kidney and adipose tissue eQTLs mapped in the GKxBN F2 cross. Eleven of the top 15 biological pathways regulated by eQTLs in kidney were also significantly altered in adipose tissue (Table 2). We found evidence of conserved biological effects of eQTLs in the two tissues for immunological functions, including autoimmune diseases (e.g. thyroid and graft versus host diseases, type 1 diabetes) and autoimmune or inflammatory mechanisms (e.g. antigen processing and presentation, phagosome, allograft rejection), as well as the metabolism of drug metabolism by cytochrome P450, butanoate, selenocompounds and several amino acids (alanine, aspartate, glutamate, valine, leucine, isoleucine). On the other hand, enrichment of eQTLs for genes involved in the metabolism of ketone bodies, steroid hormone, nitrogen, arachidonic acid, retinol, and vitamins B6 and C was significant specifically in the kidney, whereas enrichment of eQTLs for genes involved in the metabolism of fatty acid and amino acids (cysteine, methionine phenylalanine, tryptophan, tyrosine) was specific to the adipose tissue.

Common transcriptional regulation of the phagosome pathway (KEGG 4145) in both kidney and adipose tissue was mostly driven by shared strongly significant cis-eQTLs (LOD>7) linked to *RT1-A2*, *RT1-CE5*, *RT1-CE10*, *RT1-CE15*, *RT1-CE16*, *RT1-M3-1*, *RT1-T24-4*, *Cd36* and *Dync1li1* (Figure 5A). Other strongly significant eQTL genes contributing to the enrichment of this pathway were detected only in kidney (*RT1-N3*, *Atp6v0a4*, *Ctss*, *Tubb2b*, *Tlr6*) or in adipose tissue (*Fcgr2a*, *RT1-CE12*, *Clec4m*, *Atp6v1c1*). This pattern of overlapping but largely incomplete conservation of eQTL regulation of biological pathways between tissues was also observed for the metabolic regulations pathway (KEGG 1100) (Figure 5B). Consistent genetic regulation of metabolic regulations was based on only 38 consistent eQTLs in kidney and adipose tissue that co-localised in the genome and showed the same allelic effects on the direction of gene expression changes in the two tissues. The remaining eQTLs contributing to the enrichment of metabolic pathways were localised to different chromosomes, showed discordant gene expression patterns in the two tissues (n=22), or were detected specifically in kidney (n=123) (e.g. *Ugt2b*, *Cyp4a8*) or in fat (n=114) (e.g. *Cyp2e1*) (Table S4).

The valine, leucine and isoleucine degradation pathway (KEGG 280) provided a typical example of the complexity of tissue-specific genetic control of gene transcription (Table 3). Even though the pathway was consistently significantly enriched in both kidney and adipose tissue with similar numbers of contributing genes in the two tissues, the eQTL genes responsible for the enrichment showed clear tissue specific expression. Only the eQTL gene *Bckdhb* showed conserved mapping position and consistent genetic regulation of expression in kidney and adipose tissue. All other eQTL genes were either tissue-specific or mapped to different chromosomal locations in the two tissues.

These data illustrate organ-specific genetic regulation of gene transcription patterns and the involvement of distinct molecular components regulating the same pathway in different tissues in the context of type 2 diabetes and its renal complications.

Kidney and adipose tissue eQTLs mapped in the GK are conserved in the spontaneously hypertensive rat (SHR).

To test the pathophysiological relevance of our findings, we compared eQTLs mapped in the GKxBN F2 cross with those identified in a rat recombinant inbred (RI) panel derived from the spontaneously hypertensive rat (SHR) and the BN strain previously used to map eQTLs in adipose tissue and kidney (Hubner et al., 2005). Both GK and SHR are models of insulin resistance that derive from a similar outbred stock of Wistar rats selected for glucose intolerance (GK) (Goto et al., 1976) or high blood pressure (SHR) (Gauguier, 2005). eQTL comparisons in the two mapping systems were based on renal and adipose tissue eQTLs identified in the SHR:BN RI for 255 (kidney) and 203 (fat) known genes. Of these, 56 kidney eQTL genes (22%) and 52 adipose tissue eQTL genes (26%) were conserved in the BNxGK F2 cross (Table S6). The effect of GK and SHR alleles on gene transcription was consistent for 38 kidney eQTLs (68%) and 36 adipose tissue eQTLs (69%), suggesting shared genetic control of the linked genes in the two strains. On the other hand, *trans*-regulated eQTLs identified in RI strains almost systematically mapped to a different chromosome in the F2 cross and therefore underlie distinct genetic regulation (Table S6).

To further test eQTL consistency in GK and SHR, we considered genes linked to genetic markers localised in a window of 10Mb in the two mapping systems, in order to account for differences in mapping resolution of genetic markers in an F2 cross and in RI strains. Using this criterion, we identified 24 kidney eQTLs and 17 fat eQTLs that showed evidence of co-localisation in the two systems (Table 4). Of these, the majority of eQTLs were cis-mediated in kidney (n=19; 79%) and fat (n=13; 76%) and three were ambiguous in the F2 cross. We

identified only two *trans*-mediated eQTLs (*Nrd1*, *Sectm1b*) conserved in GK and SHR. Five genes (*Ascl3*, *Cd36*, *Dcps*, *Ilf3*, *Mrpl4*) were linked to eQTLs in the two tissues. In the vast majority of cases, the effects of the GK and SHR alleles on the expression of the linked genes were consistent.

These data underline similarities in the genetic regulation of gene transcription in the GK and SHR and suggest common genetic etiology of insulin resistance in both models.

Discussion

We have characterised the genetic architecture and function of the renal transcriptome in diabetes in a F2 cross derived from diabetic GK rats and normoglycemic BN controls, which we compared to adipose tissue eQTL data in the cross and transcriptome data in a panel of recombinant inbred (RI) strains derived from rats of the SHR model of spontaneous hypertension associated with insulin resistance and BN controls. We provide mapping and functional details of shared and organ-specific genetic regulation of gene expression in kidney and adipose tissue in the F2 cross. Similarities in the genetic control of gene transcription in the GK and SHR suggest shared disease etiology in these models, and provide information on molecular mechanisms and genes involved in insulin resistance and renal anomalies in the contexts of chronic hypertension and hyperglycemia.

Linkage mapping in the cross identified instances of polygenic control of renal transcripts, eQTL hotspots and sex-specific and cross direction effects (CDE), which were largely distinct to those previously reported in adipose tissue in the same cross (Kaisaki et al., 2016). Several of such eQTL features, which are dominated by transcription regulation in *trans*, have been described in many species and experimental settings (Albert et al., 2018; Hasin-Brumshtein et al., 2016; Kaisaki et al., 2016; Tian et al., 2016). Parent-of-origin effects on gene expression cannot be disentangled in F2 progenies and cannot unambiguously explain

CDE on eQTLs. Evidence of increased diabetes severity in F1 progenies of GK mothers (Gauguier et al., 1994) and the regulation of imprinted genes by CDE eQTLs in the GKxBN F2 cross suggests that parental imprinting affects the phenotypes and gene expression in the GK.

The low effect size of *trans*-mediated eQTLs is an important issue in assessing genuine sex-specific and CDE eQTLs. The impact of CDE on eQTLs has not been addressed in the context of an F2 cross. On the other hand, genotype by sex effects have been documented in QTL studies, including in the GKxBN F2 cross (Gauguier et al., 1996), and the general consensus is that they have a modest effect on eQTLs (Dimas et al., 2012; Kassam et al., 2016), so as on many physiological QTLs (Krohn et al., 2014). The definition of *cis*-mediated gene expression regulation and eQTL hotspots, which relies on arbitrary estimates of physical distances between genetic markers and linked transcripts (Breitling et al., 2008; Petretto et al., 2006), is problematic in experimental crosses and RI strains due to the extensive linkage disequilibrium preventing the high resolution mapping required to separate closely linked eQTLs. Nevertheless, our present assessment of renal eQTL hotspots and *cis*-regulated eQTLs is consistent with our previous eQTL mapping data in adipose tissue in the GKxBN F2 cross, which we validated in congenic series from the same strain combination (Kaisaki et al., 2016).

Data from our previous Illumina microarray-based renal transcriptome analyses in the GK (Hu et al., 2009; Wilder et al., 2009) provide experimental validation for a large number of kidney eQTLs. About 44% (n=589) of genes differentially expressed in the kidney between GK and BN are controlled by eQTLs in the F2 cross. These figures are consistent with our adipose tissue transcriptome data which showed that 43% (531/1221) of differentially expressed genes between GK and BN corresponded to eQTLs (Kaisaki et al., 2016). Even considering the extreme phenotypic and genomic divergence between GK and BN (Atanur et

al., 2013; Saar et al., 2008) potentially contributing to gene expression changes, as much as 26% (n=347) of differentially expressed genes in kidney between GK and Wistar Kyoto strains (Hu et al., 2009), which derive from the same outbred Wistar stock and are therefore genetically closely related, are renal eQTLs in the GKxBN F2 cross .

Genome-wide transcriptome profiling allows unbiased and systematic analyses of biological pathways. Pathways related to immunological processes, which are believed to play a role in type 2 diabetes (e.g. phagosome, cell adhesion molecules, natural killer cell mediated cytotoxicity), were significantly altered in both kidney and adipose tissue in the cross. We also noted associations with metabolic pathways (bile acids, ketone bodies, steroid hormone, arachidonic acid, leucine, isoleucine, valine) relevant to mechanisms involved in type 2 diabetes and potentially contributing to GK pathophysiology. In particular the branched-chain amino acids (BCAAs) leucine, isoleucine and valine are essential amino acids synthesized by gut bacteria (Amorim Franco and Blanchard, 2017) and are associated with insulin resistance (Newgard et al., 2009) and increased type 2 diabetes risk (Lotta et al., 2016). The identification of largely distinct series of eQTL genes independently contributing to BCAA metabolism in kidney and adipose tissue in the GKxBN F2 cross demonstrates the tissue specific genetic control of a biological function involved in diabetes. It suggests that different components of the pathway are expressed in the two tissues or that the pathway is fully expressed in the two tissues, but different components are under eQTL control.

At the gene level, our eQTL data provide information on the genetic control of transcription of individual genes that may contribute to phenotypes relevant to type 2 diabetes that we and others have mapped to the rat genome in F2 crosses and congenic strains (Bihoreau et al., 2017). We detected eQTLs for genes known to carry functional variants contributing to glucose intolerance QTLs in the GK, including the inositol polyphosphate phosphatase-like 1 (*Ship2, Inppl1*) and the insulin degradation enzyme (*Ide*) (Fakhrai-Rad et al., 2000; Marion et

al., 2002). Of direct relevance to this study, our renal eQTL data can assist the identification of genes underlying QTLs for proteinuria detected in a GKxBN F2 cross (Nobrega et al., 2009). The 1.5 LOD confidence intervals around the peaks of maximum linkage of these QTLs (approximately 77-120Mb on chromosome 5 and 60-112Mb on chromosome 7; RGSC3.4, Ensembl release 69) contain a total of 69 renal eQTLs in our GKxBN F2 cross, which represent functional and positional candidates for these proteinuria QTLs in the GK rat. Among these, the 16 cis-regulated eQTL genes localised at the proteinuria QTLs (*Abca1*, *Ambp*, *Angptl3*, *Cdk5rap2*, *Echdc2*, *Fkbp15*, *Fktn*, *Inadl*, *Laptm4b*, *Ly6c*, *Mysm1*, *Nipsnap3b*, *RGD1311188*, *RGD1564131*, *Rraga*, *Slc22a22*) are particularly relevant since sequence variants at the loci alter their expression. Of note, the glycosyltransferase fukutin (*Fktn*, eQTL LOD=8.02, P<0.001) regulates the number and structure of podocytes (Kojima et al., 2011), and the α-1-microglobulin/bikunin precursor (*Ambp*, eQTL LOD=14.53, P<0.001) is elevated in urines of patients with diabetic nephropathy (Zubiri et al., 2014). The identification of renal eQTLs for genes involved in polycystic kidney disease (*Pkd2*, *cis*-effect, LOD=19, P<0.001; *Pkdrej*, *trans*-effect, LOD=4.88, P=0.0042) provides molecular evidence of the extent of renal anomalies in the GK.

We identified similarities in eQTLs mapped in the GK and SHR. Both strains exhibit insulin resistance and renal anomalies and share an important proportion of genetic polymorphisms (Atanur et al., 2013; Saar et al., 2008), which were isolated following a process of phenotype-based selection of outbred Wistar rats. We tested the hypothesis of conserved genetic regulation of transcription in GK and SHR by comparing eQTLs mapped in kidney and adipose tissue in both GKxBN F2 rats and SHR:BN RI strains. Similar numbers of eQTL were detected in the two tissues in F2 and RI rats (Grieve et al., 2008). In both tissues, we identified a high concordance of eQTLs in GK and SHR despite differences (i) in maintenance conditions of the animals, (ii) in platforms used for transcriptome analyses

(Illumina beadchips in F2 rats, Affymetrix arrays in RI strains), (iii) in statistical methods applied to eQTL mapping and (iv) in genotype frequencies (3 genotypes in the F2 cross and either SHR or BN homozygous genotypes at all loci in RI). The latter resulted in differences in genetic mapping resolution in the F2 and RI panels, making comparisons of *cis*- and *trans*-mediated effects difficult in the two populations.

In strong support to our hypothesis of common genetic factors contributing to disease phenotypes in GK and SHR or SHR-related strains (SHRSP, SHHF), we identified eQTLs in the GK for three genes that are central to SHR etiopathogenesis, including the angiotensin I converting enzyme (*Ace*), which was the strongest candidate in the initial genetic study in the SHR (Hilbert et al., 1991), the Cd36 protein (Aitman et al., 1999) and the epoxide hydrolase 2 (*Ephx2*), which is associated with heart failure (Monti et al., 2008). We previously reported evidence of massive downregulated renal expression of *Ephx2* in the GK when compared to both BN rats (expression fold change: -11.7, $P=2.7x10^{-26}$) and Wistar Kyoto rats (expression fold change: -9.1, $P=1.1x10^{-24}$) (Hu et al., 2009). We demonstrate here the strong significance of the genetic control of its expression in the GKxBN F2 cross (LOD=91.1), where the GK alleles at the *Ephx2* locus are associated with downregulated *Ephx2* transcription. Furthermore, we identified renal eQTLs in the GKxBN F2 cross for genes directly related to *Ephx2* function, including *Ephx1* (LOD=4.3) and *Ephx4* (LOD=5.2), where the GK alleles are associated with transcription downregulation. According to the mitigating effects of *Ephx2* inactivation on renal injury induced by hyperglycemia in mice (Bettaieb et al., 2017), inhibition of its expression in the GK may underlie compensatory mechanisms to prevent renal dysfunction.

eQTL genes in the GK rat provide functional information relevant to the pathogenesis of nephropathy in type 2 diabetes and insulin resistance in humans. Compared to other chronic diseases, large scale genetic studies of diabetes kidney disease have provided little consistent

clues and replicated genes underlying the cause of the disease, even in the largest population study (van Zuydam et al., 2018). This situation underscores the importance of functional data derived from preclinical models. Knowledge of synteny conservation between rat and human genomes (Wilder et al., 2004) can be used to exploit renal eQTL data produced in the rat to annotate the function of positional candidate genes in genomic regions linked to diabetic nephropathy in humans (Imperatore et al., 1998). Renal eQTL data in the GK can also provide direct functional information to risk genes for kidney disease phenotypes identified through GWAS. Associations to glomerular filtration rate were identified for the human homologs of renal eQTL genes encoding the DEAD box polypeptide 1 (*Ddx1*) (cis-mediated, LOD=10.89, P<0.001), dipeptidase 1 (*Dpep1*) (trans-mediated, LOD=3.97, P=0.039), jun D proto-oncogene (*Jund*) (cis-mediated, LOD=7.01, P<0.001), LDL receptor-related protein 2 (*Lrp2*) (cis-mediated, LOD=5.38, P=0.003), myopalladin (*Mypn*) (trans-mediated, LOD=4.08, P=0.027), neuregulin 1 (*Nrg1*) (trans-mediated, LOD=4.76, P=0.009), origin recognition complex subunit 4 (*Orc4*) (LOD=4.07, P=0.027), tyrosine phosphatase receptor O (*Ptpro*) (cis-mediated, LOD=13.43, P<0.001) and xylulokinase, (*Xylb*) (cis-mediated, LOD=8.25, P<0.001) (Morris et al., 2019; Pattaro et al., 2016). The association with PTPRO was significant in diabetic individuals. Suggestive association was also reported between the human homolog of the trans-mediated renal eQTL gene *Abcc8* (LOD= 4.47, P=0.007) and diabetic nephropathy in patients with type 2 diabetes (Jeong et al., 2019). Finally, the involvement of EPHX2 in diabetic nephropathy was suggested in a case control study in type 2 diabetic patients (Ma et al., 2018).

Interestingly, loci associated with IgA nephropathy in humans (Kiryluk et al., 2014; Yu et al., 2011; Zhou et al., 2014) contain homologs of kidney eQTL genes in the GK encoding integrin alpha X (*Itgax*) (*cis*-regulated, LOD=8.86, P<0.001), myotubularin related protein 3 (*Mtm3*) (*trans*-regulated, LOD= 3.95, P=0.04) and tumor necrosis factor 13 (*Tnfsf13*) (*cis*-

regulated, LOD=10.87, P<0.001), suggesting that the GK strain exhibits a broad spectrum of disease phenotypes and that the GK eQTL data can contribute to enhance knowledge of molecular mechanisms involved in a wide range of human disorders.

Conclusions

GWAS of diabetes kidney disease have yet to deliver consensus causative genes of strong effect size accounting for its genetic etiology in humans. Our data provide original information on altered genetic control of renal genes and biological pathways in a preclinical model of type 2 diabetes, which spontaneously develops renal anomalies relevant to diabetes nephropathy. Conserved genetic control of transcription in kidney in diabetic GK rats and in the SHR model of hypertension associated with insulin resistance, in particular for genes causing disease phenotypes in the SHR, suggests common disease etiopathogenesis in the two strains. Our data may therefore have broad applications in the definition of molecular targets and pathways of renal structural and functional anomalies in humans beyond diabetes nephropathy.

Competing interests

The authors declare no competing interests

Funding

This work was supported by the Wellcome Trust Core Award Grant (075491/Z/04), a Wellcome Senior Fellowship in Basic Biomedical Science (057733) to D.G. and grants from the European Community`s Seventh Framework Programmes under grant agreement HEALTH-F4-2010-241504 (EURATRANS) to D.G. and the Fondation pour la Recherche Médicale (FRM, INE20091217993) to D.G.

Data availability

Microarray data have been deposited in ArrayExpress (http://www.ebi.ac.uk/arrayexpress/) under the accession number E-MTAB-969.

Authors contributions

DG conceived and designed the experiments. PJK and KA performed the gene expression profiling experiments. GWO, PJK, FB, ALL, JBC, RM and DG analyzed the data. DG wrote the manuscript.

References

Ahlqvist, E., van Zuydam, N.R., Groop, L.C., and McCarthy, M.I. (2015). The genetics of diabetic complications. Nat Rev Nephrol *11*, 277-287.

Aitman, T.J., Glazier, A.M., Wallace, C.A., Cooper, L.D., Norsworthy, P.J., Wahid, F.N., Al-Majali, K.M., Trembling, P.M., Mann, C.J., Shoulders, C.C., *et al.* (1999). Identification of Cd36 (Fat) as an insulin-resistance gene causing defective fatty acid and glucose metabolism in hypertensive rats. Nat Genet *21*, 76-83.

Albert, F.W., Bloom, J.S., Siegel, J., Day, L., and Kruglyak, L. (2018). Genetics of. Elife *7*.

Alberts, R., Terpstra, P., Li, Y., Breitling, R., Nap, J.P., and Jansen, R.C. (2007). Sequence polymorphisms cause many false cis eQTLs. PLoS One *2*, e622.

Amorim Franco, T.M., and Blanchard, J.S. (2017). Bacterial Branched-Chain Amino Acid Biosynthesis: Structures, Mechanisms, and Drugability. Biochemistry *56*, 5849-5865.

Argoud, K., Wilder, S.P., McAteer, M.A., Bihoreau, M.T., Ouali, F., Woon, P.Y., Wallis, R.H., Ktorza, A., and Gauguier, D. (2006). Genetic control of plasma lipid levels in a cross derived from normoglycaemic Brown Norway and spontaneously diabetic Goto-Kakizaki rats. Diabetologia *49*, 2679-2688.

Atanur, S.S., Diaz, A.G., Maratou, K., Sarkis, A., Rotival, M., Game, L., Tschannen, M.R., Kaisaki, P.J., Otto, G.W., Ma, M.C., *et al.* (2013). Genome Sequencing Reveals Loci under Artificial Selection that Underlie Disease Phenotypes in the Laboratory Rat. Cell *154*, 691-703.

Aylor, D.L., Valdar, W., Foulds-Mathes, W., Buus, R.J., Verdugo, R.A., Baric, R.S., Ferris, M.T., Frelinger, J.A., Heise, M., Frieman, M.B., *et al.* (2011). Genetic analysis of complex traits in the emerging Collaborative Cross. Genome Res *21*, 1213-1222.

Battle, A., Brown, C.D., Engelhardt, B.E., Montgomery, S.B., Consortium, G., Laboratory, D.t.A.C.C.L.A.W.G., Group, S.M.g.A.W., groups, E.G.e., Fund, N.C., NIH/NCI, *et al.* (2017). Genetic effects on gene expression across human tissues. Nature *550*, 204-213.

Bettaieb, A., Koike, S., Hsu, M.F., Ito, Y., Chahed, S., Bachaalany, S., Gruzdev, A., Calvo-Rubio, M., Lee, K.S.S., Inceoglu, B., *et al.* (2017). Soluble epoxide hydrolase in podocytes is a significant contributor to renal function under hyperglycemia. Biochim Biophys Acta Gen Subj *1861*, 2758-2765.

Bihoreau, M.T., Dumas, M.E., Lathrop, M., and Gauguier, D. (2017). Genomic regulation of type 2 diabetes endophenotypes: Contribution from genetic studies in the Goto-Kakizaki rat. Biochimie *143*, 56-65.

Breitling, R., Li, Y., Tesson, B.M., Fu, J., Wu, C., Wiltshire, T., Gerrits, A., Bystrykh, L.V., de Haan, G., Su, A.I., *et al.* (2008). Genetical genomics: spotlight on QTL hotspots. PLoS Genet *4*, e1000232.

Broman, K.W., Wu, H., Sen, S., and Churchill, G.A. (2003). R/qtl: QTL mapping in experimental crosses. Bioinformatics *19*, 889-890.

Davis, R.C., van Nas, A., Castellani, L.W., Zhao, Y., Zhou, Z., Wen, P., Yu, S., Qi, H., Rosales, M., Schadt, E.E., *et al.* (2012). Systems genetics of susceptibility to obesity-induced diabetes in mice. Physiol Genomics *44*, 1-13.

Dimas, A.S., Nica, A.C., Montgomery, S.B., Stranger, B.E., Raj, T., Buil, A., Giger, T., Lappalainen, T., Gutierrez-Arcelus, M., McCarthy, M.I., *et al.* (2012). Sex-biased genetic effects on gene regulation in humans. Genome Res *22*, 2368-2375.

Dixon, A.L., Liang, L., Moffatt, M.F., Chen, W., Heath, S., Wong, K.C., Taylor, J., Burnett, E., Gut, I., Farrall, M., *et al.* (2007). A genome-wide association study of global gene expression. Nat Genet *39*, 1202-1207.

Dumas, M.E., Domange, C., Calderari, S., Martínez, A.R., Ayala, R., Wilder, S.P., Suárez-Zamorano, N., Collins, S.C., Wallis, R.H., Gu, Q., *et al.* (2016). Topological analysis of

metabolic networks integrating co-segregating transcriptomes and metabolomes in type 2 diabetic rat congenic series. Genome Med *8*, 101.
Dumas, M.E., Wilder, S.P., Bihoreau, M.T., Barton, R.H., Fearnside, J.F., Argoud, K., D'Amato, L., Wallis, R.H., Blancher, C., Keun, H.C., *et al.* (2007). Direct quantitative trait locus mapping of mammalian metabolic phenotypes in diabetic and normoglycemic rat models. Nat Genet *39*, 666-672.
Fairfax, B.P., Makino, S., Radhakrishnan, J., Plant, K., Leslie, S., Dilthey, A., Ellis, P., Langford, C., Vannberg, F.O., and Knight, J.C. (2012). Genetics of gene expression in primary immune cells identifies cell type-specific master regulators and roles of HLA alleles. Nat Genet *44*, 502-510.
Fakhrai-Rad, H., Nikoshkov, A., Kamel, A., Fernström, M., Zierath, J.R., Norgren, S., Luthman, H., and Galli, J. (2000). Insulin-degrading enzyme identified as a candidate diabetes susceptibility gene in GK rats. Hum Mol Genet *9*, 2149-2158.
Falcon, S., and Gentleman, R. (2007). Using GOstats to test gene lists for GO term association. Bioinformatics *23*, 257-258.
Finlay, C., Argoud, K., Wilder, S.P., Ouali, F., Ktorza, A., Kaisaki, P.J., and Gauguier, D. (2010). Chromosomal mapping of pancreatic islet morphological features and regulatory hormones in the spontaneously diabetic (Type 2) Goto-Kakizaki rat. Mamm Genome *21*, 499-508.
Gamazon, E.R., Segrè, A.V., van de Bunt, M., Wen, X., Xi, H.S., Hormozdiari, F., Ongen, H., Konkashbaev, A., Derks, E.M., Aguet, F., *et al.* (2018). Using an atlas of gene regulation across 44 human tissues to inform complex disease- and trait-associated variation. Nat Genet *50*, 956-967.
Gauguier, D. (2005). The rat as a model physiological system., Vol 3 (Wiley).
Gauguier, D., Froguel, P., Parent, V., Bernard, C., Bihoreau, M.T., Portha, B., James, M.R., Penicaud, L., Lathrop, M., and Ktorza, A. (1996). Chromosomal mapping of genetic loci associated with non-insulin dependent diabetes in the GK rat. Nat Genet *12*, 38-43.
Gauguier, D., Nelson, I., Bernard, C., Parent, V., Marsac, C., Cohen, D., and Froguel, P. (1994). Higher maternal than paternal inheritance of diabetes in GK rats. Diabetes *43*, 220-224.
Goto, Y., Kakizaki, M., and Masaki, N. (1976). Production of spontaneous diabetic rats by repetition of selective breeding. Tohoku J Exp Med *119*, 85-90.
Grieve, I.C., Dickens, N.J., Pravenec, M., Kren, V., Hubner, N., Cook, S.A., Aitman, T.J., Petretto, E., and Mangion, J. (2008). Genome-wide co-expression analysis in multiple tissues. PLoS One *3*, e4033.
Grundberg, E., Small, K.S., Hedman, Å., Nica, A.C., Buil, A., Keildson, S., Bell, J.T., Yang, T.P., Meduri, E., Barrett, A., *et al.* (2012). Mapping cis- and trans-regulatory effects across multiple tissues in twins. Nat Genet *44*, 1084-1089.
Haley, C.S., and Knott, S.A. (1992). A simple regression method for mapping quantitative trait loci in line crosses using flanking markers. Heredity *69*, 315-324.
Hasin-Brumshtein, Y., Khan, A.H., Hormozdiari, F., Pan, C., Parks, B.W., Petyuk, V.A., Piehowski, P.D., Brümmer, A., Pellegrini, M., Xiao, X., *et al.* (2016). Hypothalamic transcriptomes of 99 mouse strains reveal trans eQTL hotspots, splicing QTLs and novel non-coding genes. Elife *5*.
Hilbert, P., Lindpaintner, K., Beckmann, J.S., Serikawa, T., Soubrier, F., Dubay, C., Cartwright, P., De Gouyon, B., Julier, C., and Takahasi, S. (1991). Chromosomal mapping of two genetic loci associated with blood-pressure regulation in hereditary hypertensive rats. Nature *353*, 521-529.
Hu, Y., Kaisaki, P.J., Argoud, K., Wilder, S.P., Wallace, K.J., Woon, P.Y., Blancher, C., Tarnow, L., Groop, P.H., Hadjadj, S., *et al.* (2009). Functional annotations of diabetes

nephropathy susceptibility loci through analysis of genome-wide renal gene expression in rat models of diabetes mellitus. BMC Med Genomics *2*, 41.
Hubner, N., Wallace, C.A., Zimdahl, H., Petretto, E., Schulz, H., Maciver, F., Mueller, M., Hummel, O., Monti, J., Zidek, V., *et al.* (2005). Integrated transcriptional profiling and linkage analysis for identification of genes underlying disease. Nat Genet *37*, 243-253.
Imperatore, G., Hanson, R.L., Pettitt, D.J., Kobes, S., Bennett, P.H., and Knowler, W.C. (1998). Sib-pair linkage analysis for susceptibility genes for microvascular complications among Pima Indians with type 2 diabetes. Pima Diabetes Genes Group. Diabetes *47*, 821-830.
Janssen, U., Vassiliadou, A., Riley, S.G., Phillips, A.O., and Floege, J. (2004). The quest for a model of type II diabetes with nephropathy: the Goto Kakizaki rat. J Nephrol *17*, 769-773.
Jeong, K.H., Kim, J.S., Woo, J.T., Rhee, S.Y., Lee, Y.H., Kim, Y.G., Moon, J.Y., Kim, S.K., Kang, S.W., Lee, S.H., *et al.* (2019). Genome-Wide Association Study Identifies New Susceptibility Loci for Diabetic nephropathy in Korean patients with type 2 diabetes mellitus. Clin Genet.
Kaisaki, P.J., Otto, G.W., Argoud, K., Collins, S.C., Wallis, R.H., Wilder, S.P., Yau, A.C., Hue, C., Calderari, S., Bihoreau, M.T., *et al.* (2016). Transcriptome Profiling in Rat Inbred Strains and Experimental Cross Reveals Discrepant Genetic Architecture of Genome-Wide Gene Expression. G3 (Bethesda).
Kassam, I., Lloyd-Jones, L., Holloway, A., Small, K.S., Zeng, B., Bakshi, A., Metspalu, A., Gibson, G., Spector, T.D., Esko, T., *et al.* (2016). Autosomal genetic control of human gene expression does not differ across the sexes. Genome Biol *17*, 248.
Kiryluk, K., Li, Y., Scolari, F., Sanna-Cherchi, S., Choi, M., Verbitsky, M., Fasel, D., Lata, S., Prakash, S., Shapiro, S., *et al.* (2014). Discovery of new risk loci for IgA nephropathy implicates genes involved in immunity against intestinal pathogens. Nat Genet *46*, 1187-1196.
Kojima, K., Nosaka, H., Kishimoto, Y., Nishiyama, Y., Fukuda, S., Shimada, M., Kodaka, K., Saito, F., Matsumura, K., Shimizu, T., *et al.* (2011). Defective glycosylation of α-dystroglycan contributes to podocyte flattening. Kidney Int *79*, 311-316.
Krohn, J., Speed, D., Palme, R., Touma, C., Mott, R., and Flint, J. (2014). Genetic interactions with sex make a relatively small contribution to the heritability of complex traits in mice. PLoS One *9*, e96450.
Lee, P.D., Ge, B., Greenwood, C.M., Sinnett, D., Fortin, Y., Brunet, S., Fortin, A., Takane, M., Skamene, E., Pastinen, T., *et al.* (2006). Mapping cis-acting regulatory variation in recombinant congenic strains. Physiol Genomics *25*, 294-302.
Lotta, L.A., Scott, R.A., Sharp, S.J., Burgess, S., Luan, J., Tillin, T., Schmidt, A.F., Imamura, F., Stewart, I.D., Perry, J.R., *et al.* (2016). Genetic Predisposition to an Impaired Metabolism of the Branched-Chain Amino Acids and Risk of Type 2 Diabetes: A Mendelian Randomisation Analysis. PLoS Med *13*, e1002179.
Ma, L., Yan, M., Kong, X., Jiang, Y., Zhao, T., Zhao, H., Liu, Q., Zhang, H., Liu, P., Cao, Y., *et al.* (2018). Association of. J Diabetes Res *2018*, 2786470.
Marion, E., Kaisaki, P.J., Pouillon, V., Gueydan, C., Levy, J.C., Bodson, A., Krzentowski, G., Daubresse, J.C., Mockel, J., Behrends, J., *et al.* (2002). The gene INPPL1, encoding the lipid phosphatase SHIP2, is a candidate for type 2 diabetes in rat and man. Diabetes *51*, 2012-2017.
Monti, J., Fischer, J., Paskas, S., Heinig, M., Schulz, H., Gösele, C., Heuser, A., Fischer, R., Schmidt, C., Schirdewan, A., *et al.* (2008). Soluble epoxide hydrolase is a susceptibility factor for heart failure in a rat model of human disease. Nat Genet *40*, 529-537.
Morris, A.P., Le, T.H., Wu, H., Akbarov, A., van der Most, P.J., Hemani, G., Smith, G.D., Mahajan, A., Gaulton, K.J., Nadkarni, G.N., *et al.* (2019). Trans-ethnic kidney function

association study reveals putative causal genes and effects on kidney-specific disease aetiologies. Nat Commun *10*, 29.
Newgard, C.B., An, J., Bain, J.R., Muehlbauer, M.J., Stevens, R.D., Lien, L.F., Haqq, A.M., Shah, S.H., Arlotto, M., Slentz, C.A., *et al.* (2009). A branched-chain amino acid-related metabolic signature that differentiates obese and lean humans and contributes to insulin resistance. Cell Metab *9*, 311-326.
Nobrega, M.A., Solberg Woods, L.C., Fleming, S., and Jacob, H.J. (2009). Distinct genetic regulation of progression of diabetes and renal disease in the Goto-Kakizaki rat. Physiol Genomics *39*, 38-46.
Pattaro, C., Teumer, A., Gorski, M., Chu, A.Y., Li, M., Mijatovic, V., Garnaas, M., Tin, A., Sorice, R., Li, Y., *et al.* (2016). Genetic associations at 53 loci highlight cell types and biological pathways relevant for kidney function. Nat Commun *7*, 10023.
Petretto, E., Mangion, J., Dickens, N.J., Cook, S.A., Kumaran, M.K., Lu, H., Fischer, J., Maatz, H., Kren, V., Pravenec, M., *et al.* (2006). Heritability and tissue specificity of expression quantitative trait loci. PLoS Genet *2*, e172.
Saar, K., Beck, A., Bihoreau, M.T., Birney, E., Brocklebank, D., Chen, Y., Cuppen, E., Demonchy, S., Dopazo, J., Flicek, P., *et al.* (2008). SNP and haplotype mapping for genetic analysis in the rat. Nat Genet *40*, 560-566.
Shi, W., Oshlack, A., and Smyth, G.K. (2010). Optimizing the noise versus bias trade-off for Illumina whole genome expression BeadChips. Nucleic Acids Res *38*, e204.
Solberg, L.C., Baum, A.E., Ahmadiyeh, N., Shimomura, K., Li, R., Turek, F.W., Churchill, G.A., Takahashi, J.S., and Redei, E.E. (2004). Sex- and lineage-specific inheritance of depression-like behavior in the rat. Mamm Genome *15*, 648-662.
Tian, J., Keller, M.P., Broman, A.T., Kendziorski, C., Yandell, B.S., Attie, A.D., and Broman, K.W. (2016). The Dissection of Expression Quantitative Trait Locus Hotspots. Genetics *202*, 1563-1574.
van Nas, A., Ingram-Drake, L., Sinsheimer, J.S., Wang, S.S., Schadt, E.E., Drake, T., and Lusis, A.J. (2010). Expression quantitative trait loci: replication, tissue- and sex-specificity in mice. Genetics *185*, 1059-1068.
van Zuydam, N.R., Ahlqvist, E., Sandholm, N., Deshmukh, H., Rayner, N.W., Abdalla, M., Ladenvall, C., Ziemek, D., Fauman, E., Robertson, N.R., *et al.* (2018). A Genome-Wide Association Study of Diabetic Kidney Disease in Subjects With Type 2 Diabetes. Diabetes *67*, 1414-1427.
Wallis, R.H., Collins, S.C., Kaisaki, P.J., Argoud, K., Wilder, S.P., Wallace, K.J., Ria, M., Ktorza, A., Rorsman, P., Bihoreau, M.T., *et al.* (2008). Pathophysiological, genetic and gene expression features of a novel rodent model of the cardio-metabolic syndrome. PLoS One *3*, e2962.
Wilder, S.P., Bihoreau, M.T., Argoud, K., Watanabe, T.K., Lathrop, M., and Gauguier, D. (2004). Integration of the rat recombination and EST maps in the rat genomic sequence and comparative mapping analysis with the mouse genome. Genome Res *14*, 758-765.
Wilder, S.P., Kaisaki, P.J., Argoud, K., Salhan, A., Ragoussis, J., Bihoreau, M.T., and Gauguier, D. (2009). Comparative analysis of methods for gene transcription profiling data derived from different microarray technologies in rat and mouse models of diabetes. BMC Genomics *10*, 63.
Yu, X.Q., Li, M., Zhang, H., Low, H.Q., Wei, X., Wang, J.Q., Sun, L.D., Sim, K.S., Li, Y., Foo, J.N., *et al.* (2011). A genome-wide association study in Han Chinese identifies multiple susceptibility loci for IgA nephropathy. Nat Genet *44*, 178-182.
Zhou, X.J., Nath, S.K., Qi, Y.Y., Cheng, F.J., Yang, H.Z., Zhang, Y., Yang, W., Ma, J.Y., Zhao, M.H., Shen, N., *et al.* (2014). Brief Report: identification of MTMR3 as a novel

susceptibility gene for lupus nephritis in northern Han Chinese by shared-gene analysis with IgA nephropathy. Arthritis Rheumatol *66*, 2842-2848.
Zubiri, I., Posada-Ayala, M., Sanz-Maroto, A., Calvo, E., Martin-Lorenzo, M., Gonzalez-Calero, L., de la Cuesta, F., Lopez, J.A., Fernandez-Fernandez, B., Ortiz, A., *et al.* (2014). Diabetic nephropathy induces changes in the proteome of human urinary exosomes as revealed by label-free comparative analysis. J Proteomics *96*, 92-102.

Tables

Table 1. Overview of kidney eQTLs detected in GKxBN F2 hybrids. Statistical models were applied to map eQTL effects using sex and cross as additive covariates (additive model), as well as eQTLs that show sex-specificity (Sex interactive) and cross direction effect (CDE). The total number of eQTLs detected is given for each chromosome. Cis-regulated eQTL are those mapped within 10Mb of the linked transcript. Genetic effects were defined as trans-regulated eQTLs when eQTL markers and target transcripts map to different chromosomes. Chromosome length and number of protein-coding genes are based on ENSEMBL annotations of the rat genome (RGSC3.4, Ensembl release 69). Full details of genes associated with eQTLs are given in Table S1. Details of comparative analyses with published adipose tissue eQTLs mapped in the same cross (Kaisaki et al., 2016) are in Tables S4 and S5.

chr	Length (Mb)	Gene density	eQTLs	Frequency	Cis	Trans	Sex-specific	CDE
1	267.9	3030	292	0.10	105	119	35	17
2	258.2	1488	156	0.10	79	44	18	15
3	171.1	1810	118	0.07	61	40	29	9
4	187.1	1501	173	0.11	65	82	27	17
5	173.1	1405	379	0.27	89	252	116	28
6	147.6	960	96	0.10	46	29	17	6
7	143.0	1390	162	0.12	60	87	11	4
8	129.0	1241	186	0.15	82	91	18	16
9	113.4	762	175	0.23	41	111	90	18
10	110.7	1722	132	0.08	87	32	9	5
11	87.8	615	40	0.07	13	16	9	6
12	46.8	606	79	0.13	36	38	3	10
13	111.2	699	72	0.10	32	33	10	3
14	112.2	796	83	0.10	37	40	3	7
15	109.8	818	49	0.06	18	23	8	10
16	90.2	653	57	0.09	27	23	21	14
17	97.3	700	65	0.09	43	11	65	5
18	87.3	550	40	0.07	23	8	8	2
19	59.2	585	54	0.09	25	20	7	4
20	55.3	621	90	0.14	56	29	11	13
X	160.7	1028	28	0.03	4	13	0	0
Total	2718.9	22980	2526	0.11	1029	1141	515	209

Table 2. KEGG pathways significantly affected in kidney transcriptomes in the GKxBN F2 cross. Data were analysed with sex and cross as additive covariates. Data were compared to pathways altered in adipose tissue transcriptome in the same cross and reported in (Kaisaki et al., 2016). Details of pathways can be found at http://www.genome.jp/kegg/. The top 15 pathways in each tissue are highlighted. ns, not statistically significant.

KEGGID	Term	Size	Kidney			Adipose tissue		
			Count	P	Rank	Count	P	Rank
982	Drug metabolism - cytochrome P450	49	24	<0.01	1	13	0.03	25
4612	Antigen processing and presentation	60	24	<0.01	2	22	<0.01	5
980	Metabolism of xenobiotics by cyt P450	40	18	<0.01	3	-	ns	-
5416	Viral myocarditis	61	21	<0.01	4	24	<0.01	4
5332	Graft-versus-host disease	35	14	<0.01	5	17	<0.01	1
4145	Phagosome	123	34	<0.01	6	41	<0.01	2
1100	Metabolic pathways	816	163	<0.01	7	167	<0.01	9
5320	Autoimmune thyroid disease	38	14	<0.01	8	16	<0.01	7
5330	Allograft rejection	38	14	<0.01	9	16	<0.01	6
120	Primary bile acid biosynthesis	10	6	<0.01	10	-	ns	-
4940	Type I diabetes mellitus	43	15	<0.01	11	18	<0.01	3
4975	Fat digestion and absorption	25	10	<0.01	12	9	0.03	27
5140	Leishmaniasis	51	16	0.01	13	19	<0.01	10
983	Drug metabolism - other enzymes	34	12	0.01	14	-	ns	-
40	Pentose and glucuronate interconversions	19	8	0.01	15	-	ns	-
65	Butanoate metabolism	19	8	0.01	16	7	0.02	18
5323	Rheumatoid arthritis	57	17	0.01	17	-	ns	-
72	Synthesis and degradation of ketone bodies	6	4	0.01	18	-	ns	-
140	Steroid hormone biosynthesis	36	12	0.01	19	-	ns	-
53	Ascorbate and aldarate metabolism	17	7	0.01	20	-	ns	-

910	Nitrogen metabolism	17	7	0.01	21	-	ns	-
4514	Cell adhesion molecules	99	25	0.01	22	29	<0.01	8
514	Other types of O-glycan biosynthesis	25	9	0.01	23	-	ns	-
250	Alanine, aspartate, glutamate metabolism	21	8	0.01	24	9	0.01	14
790	Folate biosynthesis	7	4	0.02	25	4	0.02	20
4610	Complement and coagulation cascades	53	15	0.02	26	-	ns	-
590	Arachidonic acid metabolism	44	13	0.02	27	-	ns	-
3320	PPAR signaling pathway	58	16	0.02	28	-	ns	-
280	Valine, leucine and isoleucine degradation	36	11	0.02	29	12	0.01	15
830	Retinol metabolism	36	11	0.02	30	-	ns	-
4146	Peroxisome	65	17	0.03	31	-	ns	-
4972	Pancreatic secretion	70	18	0.03	32	-	ns	-
4640	Hematopoietic cell lineage	51	14	0.03	33	15	0.02	24
5144	Malaria	33	10	0.03	34	11	0.02	21
750	Vitamin B6 metabolism	5	3	0.03	35	-	ns	-
5150	Staphylococcus aureus infection	29	9	0.03	36	12	0.01	13
4142	Lysosome	98	23	0.04	37	-	ns	-
2010	ABC transporters	34	10	0.04	38	-	ns	-
5340	Primary immunodeficiency	21	7	0.04	39	-	ns	-
450	Selenocompound metabolism	13	5	0.05	40	5	0.04	28
270	Cysteine and methionine metabolism	27	-	ns	-	9	0.03	26
4512	ECM-receptor interaction	57	-	ns	-	15	0.05	30
71	Fatty acid metabolism	33	-	ns	-	11	0.02	19
4650	Natural killer cell mediated cytotoxicity	70	-	ns	-	19	0.02	23
511	Other glycan degradation	14	-	ns	-	6	0.02	22
360	Phenylalanine metabolism	9	-	ns	-	5	0.01	16
4970	Salivary secretion	57	-	ns	-	15	0.05	29
5322	Systemic lupus erythematosus	59	-	ns	-	19	<0.01	11
380	Tryptophan metabolism	27	-	ns	-	11	<0.01	12
350	Tyrosine metabolism	16	-	ns	-	7	0.01	17

Table 3. Detailed analysis of eQTLs contributing to the enrichment of the valine, leucine and isoleucine degradation pathway in kindey and adipose tissue in the GKxBN F2 cross. The genetic localisation (cM) of eQTLs showing the stongest linkage to the genes is dervied from their mapping position in the genetic map constructed in the GKxBN F2 cross. *The allele from either the Brown-Norway (BN) of the Goto-Kakizaki (GK) strain contributing to enhanced gene expression is reported. Chr, chromosome; ns, not statistically significant.

eQTL gene details			Kidney eQTLs				Adipose tissue eQTLs			
Symbol	Description	Chr	chr (cM)	Allele*	LOD	P	chr (cM)	Allele*	LOD	P
Abat	4-aminobutyrate aminotransferase	10	10 (4.8)	BN	4.76	0.005	-	-	ns	ns
Acaa1a	Acetyl-Coenzyme A acyltransferase 1A	8	-	-	ns	ns	4 (56.3)	BN	9.85	<0.001
			-	-	ns	ns	17 (6.1)	GK	3.99	0.046
Acat3	Acetyl-Coenzyme A acetyltransferase 3	1	-	-	ns	ns	1 (81.9)	BN	4.09	0.022
Aldh1a1	Aldehyde dehydrogenase 1 family, member A1	1	-	-	ns	ns	1 (116.9)	BN	7.25	<0.001
Aldh1a7	Aldehyde dehydrogenase family 1, subfamily A7	1	-	-	ns	ns	1 (116.2)	GK	4.52	0.016
Aldh1b1	Aldehyde dehydrogenase 1 family, member B1	5	5 (30.0)	BN	12.54	<0.001	-	-	ns	ns
Aox1	Aldehyde oxidase 1	9	9 (27.4)	BN	3.74	0.046	9 (49.9)	GK	20.33	<0.001
Aox3l1	Aldehyde oxidase 3-like 1	9	6 (45.0)	GK	3.93	0.043	-	-	ns	ns
Bcat2	Branched chain aminotransferase 2, mitochondrial	1	-	-	ns	ns	4 (52.5)	BN	5.82	0.001
Bckdhb	Branched chain keto acid dehydrogenase E1, beta	8	8 (55.1)	BN	34.3	<0.001	8 (57.5)	BN	16.84	<0.001
Dbt	Dihydrolipoamide branched chain transacylase E2	2	-	-	ns	ns	1 (54.4)	BN	4.02	0.042
Echs1	Enoyl CoA hydratase, short chain, 1, mitochondrial	1	-	-	ns	ns	1 (93.4)	BN	4.49	0.015
Hadha	Hydroxyacyl-CoA dehydrogenase, alpha subunit	6	9 (69.9)	BN	4.15	0.025	6 (10.3)	BN	7.34	<0.001
Hadhb	Hydroxyacyl-CoA dehydrogenase, beta subunit	6	6 (10.0)	GK	6.74	<0.001	-	-	ns	ns
Hmgcs1	3-hydroxy-3-methylglutaryl-CoA synthase 1	2	4 (42.5)	GK	3.85	0.043	2 (26.4)	BN	5.73	<0.001
Hmgcs2	3-hydroxy-3-methylglutaryl-CoA synthase 2	2	19 (45)	GK	4.79	0.005	-	-	ns	ns
Ivd	Isovaleryl-CoA dehydrogenase	3	3 (69.9)	BN	14.42	<0.001	-	-	ns	ns
Mccc1	Methylcrotonoyl-CoA carboxylase 1 (alpha)	2	2 (56.4)	GK	9.8	<0.001	1 (93.4)	BN	4.02	0.033
Pccb	Propionyl CoA carboxylase, beta polypeptide	8	8 (70.0)	BN	9.16	<0.001	-	-	ns	ns

Table 4. Conserved eQTLs mapped in both GKxBN F2 rats and in SHR:BN recombinant inbred (RI) strains. Data are reported for eQTL markers co-localised within a window of 10Mb in kidney and white adipose tissue (WAT) in the two mapping panels regardless of cis- and trans-mediated effects and allelic effects. The chromosome (Chr) location of the gene and the linked eQTLs are given alongwith the cis- and tans-mediated effects when unambiguously determined according to criteria used in the studies. The driving allele corresponds to the allele of the strain stimulating the transcription of the eQTL gene. Information of all eQTL genes shared in the two mapping panels in the two tissues are given in table S6.

	Gene			eQTL GKxBN F2					eQTL SHR:BN RI				
Tissue	Symbol	Description	Chr	Illumina Probe	Marker	Chr	Effect	Driving allele	Affymetrix Probeset	Marker	Chr	Effect	Driving allele
Kidney	Ascl3	Achaete-scute complex homolog 3	1	450735	c1.loc85	1	-	BN	1371085_at	D1Rat356	1	Cis	BN
Kidney	Bphl	Biphenyl hydrolase-like	17	5690025	c17.loc22.5	17	Cis	GK	1388617_at	D17Rat144	17	Cis	SHR
Kidney	Cd36	CD36 molecule	4	5550025	D4Got18	4	Cis	BN	1386901_at	Cd36	4	Cis	BN
Kidney	Dcps	Decapping enzyme, scavenger	8	3610239	D8Got43	8	Cis	BN	1374583_at	D8Rat219	8	Cis	SHR
Kidney	Dgat2	Diacylglycerol O-acyltransferase 2	1	5270347	D1Mgh20	1	Cis	GK	1371615_at	D1Rat47	1	Cis	SHR
Kidney	Dnmbp	Dynamin binding protein	1	3840711	c1.loc130	1	-	BN	1372650_at	D1Rat235	1	Trans	BN
Kidney	Ext2	Exostoses 2	3	4280053	D3Wox33	3	Cis	GK	1371611_at	D3Rat29	3	Cis	BN
Kidney	Fmod	Fibromodulin	13	4120168	D13Wox9	13	Cis	BN	1367700_at	D13N2	13	Trans	BN
Kidney	Foxred1	FAD-dependent oxidoreductase 1	8	1580358	c8.loc27.5	8	Cis	BN	1376921_at	D8Rat219	8	Cis	BN
Kidney	Gpm6a	Glycoprotein m6a	16	2680131	c16.loc12.5	16	Cis	GK	1373773_at	D16Mit1	16	Trans	SHR
Kidney	Il18	Interleukin 18	8	1660494	D8M9Mit162	8	Cis	GK	1369665_at	D8Mit12	8	Cis	SHR
Kidney	Ilf3	Interleukin enhancer binding factor 3	8	1230142	c8.loc10	8	Cis	GK	1387366_at	D8Rat68	8	Cis	SHR
Kidney	Mfap3	Microfibrillar-associated protein 3	10	7040168	D10Got64	10	Cis	GK	1390063_at	D10Rat166	10	Cis	BN
Kidney	Mrpl4	Mitochondrial ribosomal protein L4	8	870136	c8.loc10	8	Cis	BN	1388366_at	D8Rat68	8	Cis	BN
Kidney	Nfyc	Nuclear transcription factor-Y	5	6200487	c5.loc62.5	5	Cis	BN	1398268_at	D5Rat169	5	Cis	BN

Kidney	Nup133	Nucleoporin 133	19	6980739	c19.loc37.5	19	Cis	BN	1375071_at	D19Cebrp150	19	Cis	BN
Kidney	Ppm1a	Protein phosphatase 1A,	6	7100131	D6Mit8	6	Cis	GK	1368859_at	D6Rat165	6	Cis	SHR
Kidney	Prnp	Prion protein	3	2760292	c3.loc62.5	3	Cis	GK	1370156_at	D3Rat159	3	Cis	SHR
Kidney	RGD1306001	Similar to 2210021J22Rik protein	7	1410592	c7.loc80	7	Cis	BN	1371749_at	D7Rat129	7	Cis	BN
Kidney	Rtel1	Regulator of telomere elongation 1	3	2970750	c3.loc107.5	3	Cis	GK	1374921_at	D3Rat1	3	Cis	SHR
Kidney	Sectm1b	Secreted and transmembrane 1B	10	6110324	c7.loc7.5	7	Trans	GK	1376976_at	D7Rat35	7	Trans	SHR
Kidney	Snhg8	Small nucleolar RNA host gene 8	16	1580364	D16Rat11	16	Cis	GK	1390435_at	D16Rat87	16	Cis	SHR
Kidney	Tf	Transferrin	8	3190022	c8.loc72.5	8	Cis	GK	1370228_at	D8Rat123	8	Cis	SHR
Kidney	Tnfsf12	TNF ligand superfamily member 12	10	2690717	D10Wox12	10	Cis	BN	1372503_at	Abpa	10	Cis	BN
WAT	Aox1	Aldehyde oxidase 1	9	2360093	c9.loc47.5	9	Cis	GK	1387376_at	D9Rat93	9	Cis	SHR
WAT	Ascl3	Achaete-scute complex homolog 3	1	450735	c1.loc85	1	-	BN	1371085_at	D1Rat356	1	Cis	BN
WAT	Bccip	BRCA2 and CDKN1A interacting	1	5340408	c1.loc82.5	1	-	BN	1371945_at	D1Rat47	1	Trans	BN
WAT	Ccdc77	Coiled-coil domain containing 77	4	2480270	c4.loc70	4	Cis	GK	1390284_at	D4Rat202	4	Cis	SHR
WAT	Cd36	CD36 molecule	4	5550025	D4Got18	4	Cis	BN	1386901_at	Cd36	4	Cis	BN
WAT	Dcps	Decapping enzyme, scavenger	8	3610239	c8.loc30	8	Cis	BN	1390185_at	D8Rat219	8	Cis	BN
WAT	Dpt	Dermatopontin	13	5860279	c13.loc27.5	13	-	GK	1371732_at	D13Rat131	13	Cis	SHR
WAT	Eci2	Enoyl-Coenzyme A delta isomerase 2	17	6860193	D17Rat67	17	Cis	BN	1388908_at	D17Rat144	17	Cis	BN
WAT	Fmo3	Flavin containing monooxygenase 3	13	1410309	c13.loc32.5	13	Cis	GK	1368304_at	D13Mit3	13	Cis	SHR
WAT	Fut4	Fucosyltransferase 4	8	3140619	c8.loc7.5	8	Cis	GK	1373838_at	D8Utr3	8	Cis	SHR
WAT	Ilf3	Interleukin enhancer binding factor 3	8	1230142	c8.loc7.5	8	Cis	GK	1387366_at	D8Rat68	8	Cis	SHR
WAT	Itga1	Integrin, alpha 1	2	5220082	c2.loc22.5	2	Cis	GK	1387144_at	D2Rat201	2	Cis	BN
WAT	Mrpl4	Mitochondrial ribosomal protein L4	8	870136	c8.loc7.5	8	Cis	BN	1388366_at	D8Rat68	8	Cis	BN
WAT	Nqo2	NAD(P)H dehydrogenase, quinone 2	17	2680471	c17.loc27.5	17	Cis	BN	1374959_at	D17Mit2	17	Cis	BN
WAT	Nrd1	Nardilysin 1	5	3840202	c1.loc47.5	1	Trans	GK	1377340_at	D1Rat27	1	Trans	SHR
WAT	Prrc1	Proline-rich coiled-coil 1	18	4920452	D18Wox10	18	Cis	GK	1374560_at	D18Rat55	18	Cis	SHR
WAT	Slc7a7	Solute carrier family 7, member 7	15	6770113	c15.loc27.5	15	Cis	GK	1387808_at	D15Rat6	15	Cis	SHR

Figures

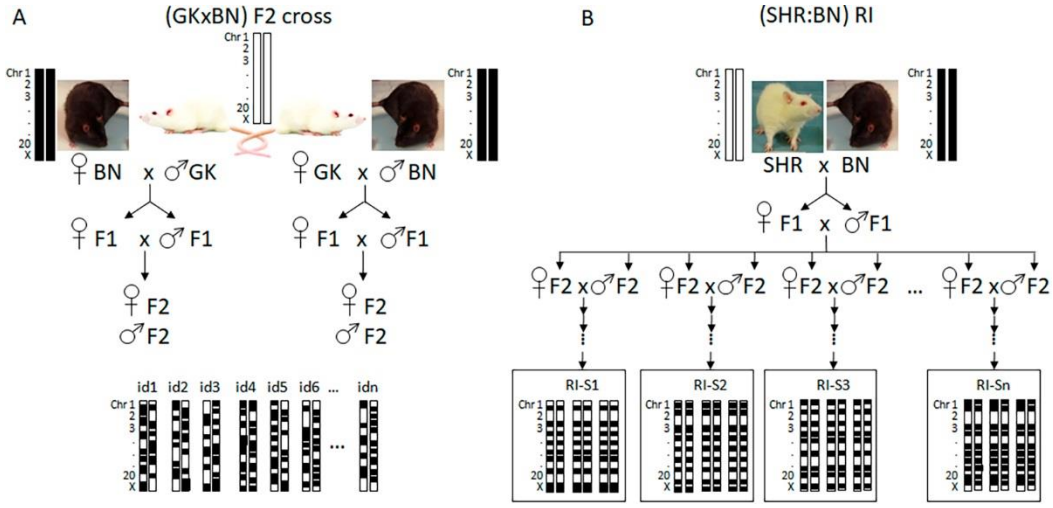

Figure 1. Breeding design applied to map eQTLs in the Goto Kakizaki rat strain. Reciprocal genetic crosses between male and female Goto Kakizaki (GK) and Brown Norway (BN) rats used to produce individual (GKxBN) F2 rats are illustrated (A) and compared to the breeding scheme designed to derive recombinant inbred strains (RI-S) from spontaneously hypertensive rats (SHR) and BN rats (B).

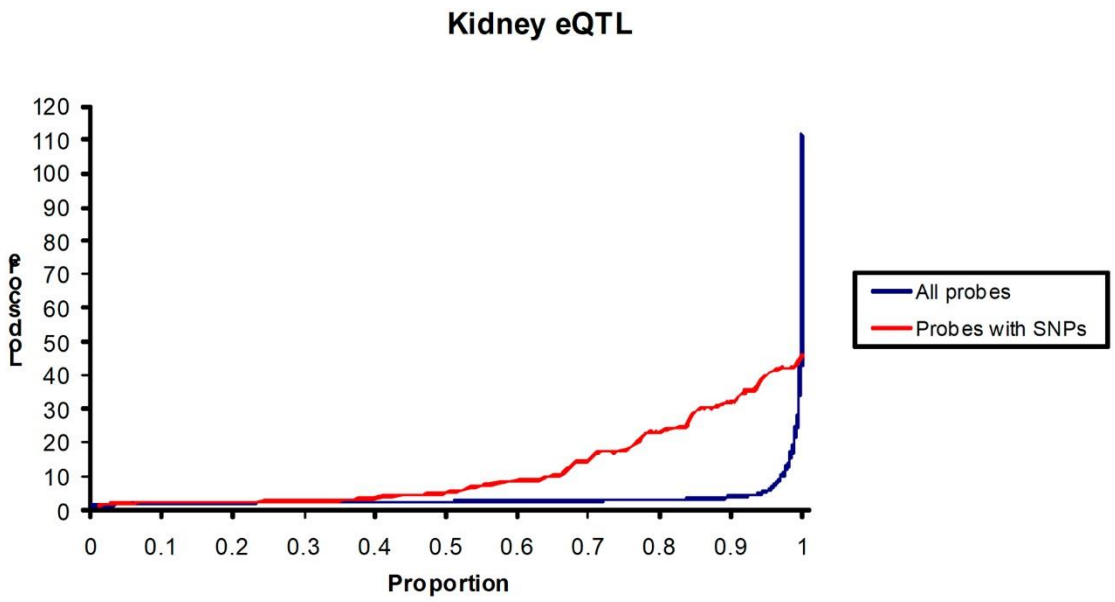

Figure 2. Distribution LOD scores for renal eQTLs mapped in the GKxBN F2 cross. LOD scores are plotted against the proportion of eQTLs detected with all Illumina oligonucleotides (blue line) and those containing DNA variation between GK and BN strains (red line).

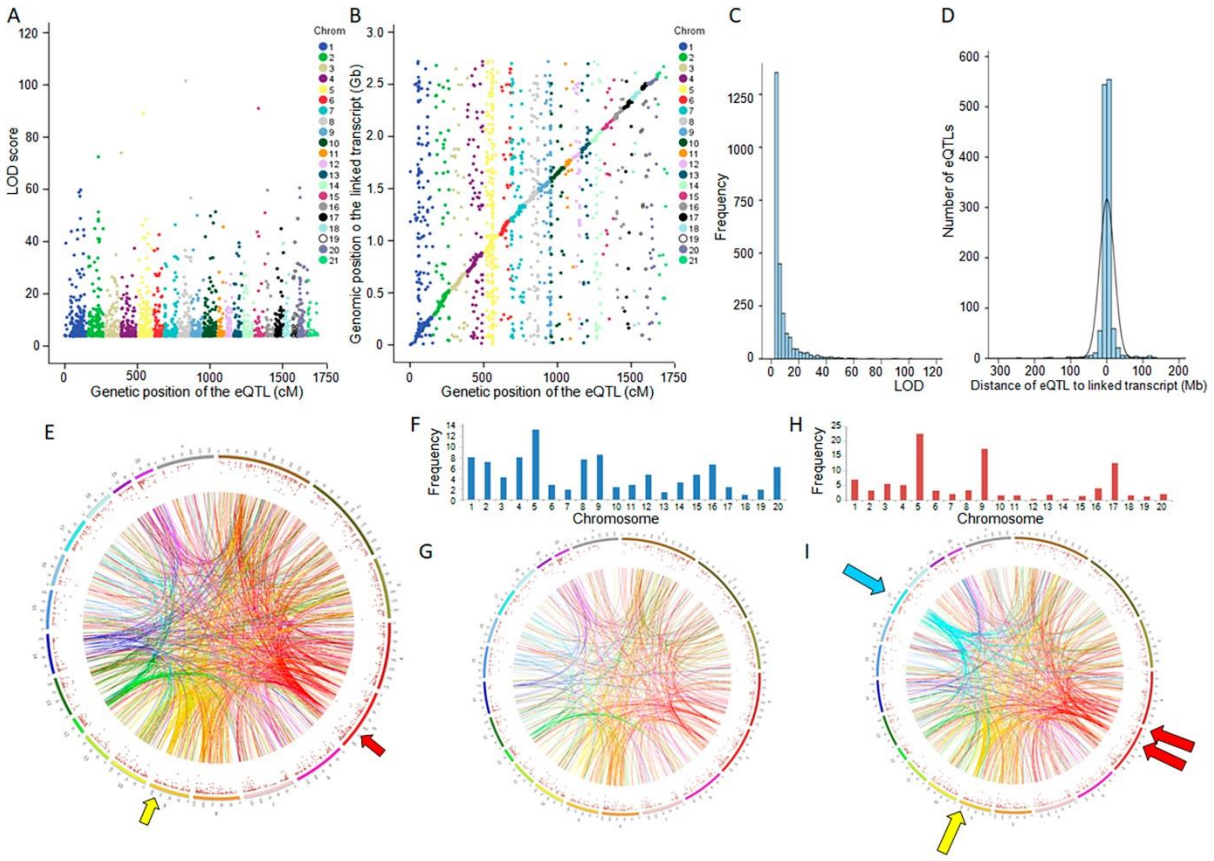

Figure 3. Kidney eQTL architecture in GKxBN F2 hybrids. Genetic positions of statistically significant eQTLs (FDR p-value<0.05) are plotted against the LOD scores (**A**). Local and distant eQTLs are illustrated by plotting genetic positions of statistically significant eQTLs and the genomic position of the linked transcripts (**B**). Distribution of LOD scores for significant eQTLs is shown (**C**). Genome mapping of pairs of eQTL and linked transcripts localised in the same chromosomes was used determine relationships between statistical significance of genetic linkage and genomic distances between transcripts and genetic markers (**D**). Mapping data from pairs of transcripts and eQTLs localised to different chromosomes illustrate distant (*trans*) effects of genetic loci on gene transcription and eQTL hotspots (arrows) (**E**). Chromosomal distribution and genome-wide trans-mediated regulation of cross direction effect (CDE) (**F,G**) and sex-specific (**H,I**) eQTLs are shown.

Chromosomes are color coded on the circle to illustrate the effects of eQTLs mapped to the same chromosomes on the expression of distant genes. Arrows indicate genomic regions of eQTL enrichment. Details of eQTLs are given in Tables S1 and S2.

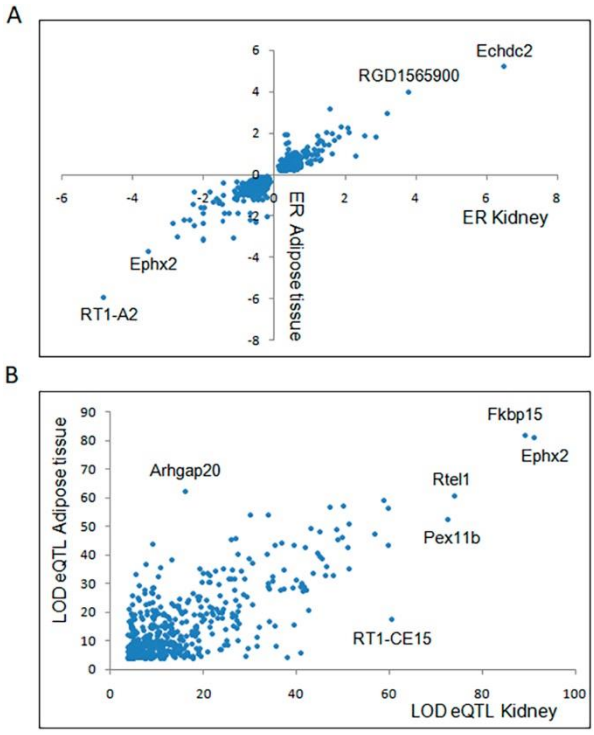

Figure 4. Comparative analyses of kidney and adipose tissue eQTLs mapped in the GKxBN F2 cross. The effect of GK alleles at the eQTLs (Expression ratio, ER) on gene expression (A) and eQTL statistical significance (LOD score) (B) in kidney and adipose tissue were plotted to illustrate the strong conservation of eQTLs detected in both tissues. Full details of statistically significant eQTLs illustrating shared and tissue specific genetic regulation of gene expression are given in Table S4.

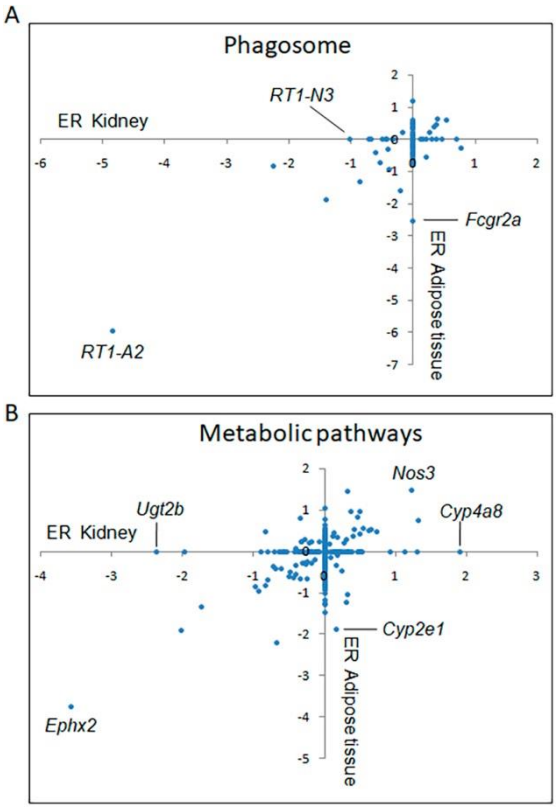

Figure 5. Tissue-specific contribution of eQTL genes to pathways enriched in both kidney and adipose tissue. Expression ratio (ER) of eQTL genes contributing to significant enrichment of phagosome and metabolic pathways in kidney and white adipose tissue are plotted to illustrate tissue specific and conserved effects of segregating GK alleles in the GKxBN F2 cross on eQTL gene transcription regulation. Full details of statistically significant eQTLs illustrating shared and tissue specific genetic regulation of gene expression are given in Table S4.

Table S1. Details of kidney eQTLs mapped in the GKxBN F2 cross. The additive model taking sex and cross into account was used to assess eQTL statistical significance. Cis-regulated eQTLs correspond to evidence of significant linkages between markers mapped within 10Mb to the linked transcript. The position (Mb) of the genes is based on ENSEMBL annotations of the rat genome (RGSC3.4, Ensembl release 69).

Click here to Download Table S1

Table S2. Details of renal eQTLs mapped in the GKxBN F2 cross showing statistical evidence of sex or cross direction effects. The position of the markers (cM) and linked genes (bp) are based on the genetic map constructed in the cross and ENSEMBL annotations of the rat genome (RGSC3.4, Ensembl release 69). chr, chromosome.

Click here to Download Table S2

Table S3. Comparative analysis of eQTLs detected in the kidney and adipose tissue in GKxBN F2 hybrids. Statistical models were applied to map eQTL effects using sex and cross as additive covariates (additive model), as well as eQTLs that show sex-specificity (Sex interactive) and cross direction effect (CDE). The total number of eQTLs detected is given for each chromosome. Cis-regulated eQTL are those mapped within 10Mb of the linked transcript. Genetic effects were defined as trans-regulated eQTLs when eQTL markers and target transcripts map to different chromosomes. Shared eQTLs were significant in both kidney and fat and showed conserved transcriptional effects of GK alleles at the eQTL. Chromosome length and number of protein-coding genes are based on ENSEMBL annotations of the rat genome (RGSC3.4, Ensembl release 69). Full details of genes associated with kidney eQTLs are given in Supplementary Table 2. Details of the sex-specific eQTLs and CDE eQTLs in the adipose tissue are supplementary table 6. Chrom, Chromosome. * Data published in Kaisaki et al., G3 6(11):3671-3683, 2016.

Click here to Download Table S3

Table S4. Details of comsistent eQTLs mappedin kidney and adiposet tissue in the GKxBN F2 cross. The additive model taking sex and cross into account was used to assess eQTL statistical significance. Cis-regulated eQTLs correspond to evidence of significant linkages between markers mapped within 10Mb to the linked transcript. The position (Mb) of the genes is based on ENSEMBL annotations of the rat genome (RGSC3.4, Ensembl release 69).

Click here to Download Table S4

Table S5. Details of adipose tissue eQTLs mapped in the GKxBN F2 cross showing statistical evidence of sex or cross direction effect. The position (Mb) of the markers and linked genes are based on ENSEMBL annotations of the rat genome (RGSC3.4, Ensembl release 69). Cis-regulated eQTLs correspond to evidence of significant linkages between markers mapped within 10Mb to the linked transcript. eQTL genes showing evidence of both sex or cross direction effect are highlighted in green. NS, Not statistically significant.

Click here to Download Table S5

Table S6. Comparative analysis of kidney and adipose tissue eQTLs mapped in the GKxBN F2 cross and in SHR:BN recombinant inbred strains

Click here to Download Table S6